Cement & Concrete Composites 55 (2015) 281–289

Contents lists available at ScienceDirect

Cement & Concrete Composites

journal homepage: www.elsevier.com/locate/cemconcomp

Effect of sodium carboxymethyl celluloses on water-catalyzed self-degradation of 200 °C-heated alkali-activated cement

T. Sugama [1], T. Pyatina *

Brookhaven National Laboratory, Building 734, Brookhaven Ave., Upton, NY 11973, USA

ARTICLE INFO

Article history:
Received 18 April 2013
Received in revised form 18 February 2014
Accepted 22 September 2014
Available online 13 October 2014

Keywords:
Sodium carboxymethyl cellulose
Enhanced geothermal system
Self-degradation
Alkali-activated cement
Fly ash
Slag

ABSTRACT

This paper investigates the usefulness of sodium carboxymethyl celluloses (CMC) in promoting self-degradation of 200 °C-heated sodium silicate-activated slag/Class C fly ash cementitious material after contact with water. CMC emitted two major volatile compounds, CO_2 and acetic acid, creating a porous structure in cement. CMC also reacted with NaOH from sodium silicate to form three solid reaction products, disodium glycolate salt, sodium glucosidic salt, and sodium bicarbonate. Other solid reaction products, such as sodium polysilicate and sodium carbonate, were derived from hydrolysates of sodium silicate. Dissolution of these products upon contact with water generated heat that promoted cement's self-degradation. Thus, CMC of high molecular weight rendered two important features to the water-catalyzed self-degradation of heated cement: one was the high heat generated in exothermic reactions in cement; the other was the introduction of extensive porosity into cement.

1. Introduction

To increase hot water or steam production the geothermal reservoirs are usually constructed in highly permeable formations that are poorly consolidated, naturally fractured or undergo through stimulation operations where large volumes of water are forced into the hot formation to open existing and create new fractures [1,2]. Consequently, lost circulation, when drilling fluid is partially or completely lost into the formation, is a common problem during construction of geothermal wells. Temporary sealing materials address this issue by plugging the fractures during the drilling operations and opening them later by disintegration when the drilling is completed.

Presently, Ordinary Portland Cement (OPC) is used as a well-casing cementing material; it is also often adapted as the binder in the sealing systems [3,4]. The major drawback of OPC use in corrosive geothermal wells is its limited resistance to the hot acidic environment created by the combination of concentrated dihydrogen sulfide (H_2S) and carbon dioxide (CO_2). As is well documented [5,6], the capacity of OPCs to withstand acid is very poor, and they suffer from severe acid erosion. To deal with this problem, acid-resistant cements are required. Alkali-activated cementitious materials (AACMs) prepared from industrial by-products with pozzolanic properties such as granulated blast-furnace slag and sodium silicate with various molar ratios of Na_2O/SiO_2, as alkali activators of pozzolanic reactions, have low susceptibility to acid erosion [7,8].

The present work evaluates potential of these AACMs as temporary sealers for geothermal wells.

The drilling temperatures of geothermal wells seldom exceed 116 °C [9] with an average temperature being around 85 °C due to the cooling effect of circulating fluids. However, well temperature rises up to more than 200 °C under static conditions, when the drilling is completed. The ideal sealer must not only plug the fractures at a low temperature of 85 °C, but also it must self-degrade at the well temperature of $\geqslant$200 °C. In hot geothermal wells the sealer plugging the fractures may encounter two different environments: one is hydrothermal at the inlet of fracture; the other is hot and dry at its end. Thus, the sealer is required to disintegrate both in hot water at 200 °C and when coming in contact with water during stimulation operations after the dry heat of 200 °C.

Several biodegradable biopolymers are currently employed as additives for cements self-degradation; they include starch, cellulose acetate, gelatin, and poly(L-lactic acid) in the form of powder, microsphere, and fiber. All of them promote the partial biological degradation of biocompatible bone cements [10–15]. When these bone-cement additives come in contact with body fluids, they degrade, creating an interconnected pore network structure in the cement, allowing the bone-tissues to grow into the channels facilitating the cement degradation. For applications in geothermal wells, of particular interest is polymers' thermal degradation. The

* Corresponding author. Tel.: +1 631 344 8646.
E-mail addresses: sugama@bnl.gov (T. Sugama), tpyatina@bnl.gov (T. Pyatina).
[1] Tel.: +1 631 344 4029.

http://dx.doi.org/10.1016/j.cemconcomp.2014.09.015
0958-9465/

cellulose and cellulose-related compounds are degraded thermally in air at around 200 °C, yielding volatile CO_2 gas and acetic acid vapor [16–18]. Sodium carboxymethyl cellulose (CMC) and cellulose-related compounds are frequently used as additives in water-based drilling fluids to reduce fluid loss and to assure desirable rheological properties at elevated temperature [19–22]. Appropriate decomposition temperature along with the compatibility with drilling fluid make carboxymethyl cellulose to be a potential candidate for modifying the AACMs system for temporarily sealing applications. This study assesses the ability of CMCs of different molecular weights to degrade the 200 °C-heated AACMs after contact with water. The tested AACMs system of slag/Class C fly ash blend was activated with sodium silicate.

2. Experimental procedure

2.1. Materials

The four different sodium carboxymethyl celluloses (CMCs) evaluated for their ability to degrade sealing material were supplied by Dow Chemical Corporation under the commercial names "Walcocel CRT 30 PA, 100 PA, 2000 PA and 30,000 PA". Two industrial by-products, possessing pozzolanic properties, were used as the hydraulic pozzolana cement: granulated blast-furnace slag under the trade name "New Cem" and Class C fly ash. The slag was supplied by Lafarge North America, and the fly ash was obtained from Boral Material Technologies, Inc. Their chemical compositions detected by micro energy-dispersive X-ray spectrometer (μEDX) were as follows: Slag; 38.5 wt% CaO, 35.2 wt% SiO_2, 12.6 wt% Al_2O_3, 10.6 wt% MgO, 1.1 wt% Fe_2O_3, and 0.4 wt% TiO_2; Class C fly ash; 30.2 wt% CaO, 31.9 wt% SiO_2, 21.7 wt% Al_2O_3, 4.6 wt% MgO, 6.1 wt% Fe_2O_3, 1.7 wt% Na_2O, 0.7 wt% K_2O_3, and 3.1 wt% SO_3. An anhydrous sodium silicate granular powder under the trade name "Metso Beads 2048," supplied by the PQ Corporation, was used as the alkali activator of these pozzolana cements; its chemical composition was 50.5 wt% Na_2O and 46.6 wt% SiO_2. The formula of the dry pozzolana cements employed in this test had slag/Class C fly ash ratio of 20/80 by weight. A 10% of this alkali activator by total weight of pozzolana cement was added to prepare the dry mix cementitious reactant. Further, 1.2% CMC by the total weight of pozzolana cement was incorporated into this dry mix. In preparing cement slurry with similar consistency, the water/blend (w/b) ratio depended on the particular CMC; namely, the ratio was 0.33, 0.39, 0.51, and 0.75, respectively, for 30 PA-, 100 PA-, 2000 PA-, and 30,000 PA-incorporated cement slurries. Higher molecular weight CMCs increased slurries' viscosities and required larger water amounts to be mixable. These slurries were left at room temperature in air for 72 h. Afterward, all set cements were autoclaved hydrothermally at 85 °C for 24 h under a pressure of 1000 psi. Since the ideal sealer not only plugs the fractures at 85 °C, but also self-degrades when the well temperature reaches ⩾200 °C, some 85 °C-autoclaved cements were further heated for 24 h in an oven at 200 °C. The heated samples were further exposed to water to simulate the stimulation operations when the sealer is expected to disintegrate.

To evaluate the susceptibility of CMCs to alkaline cement slurry at 85 and 200 °C, the cement pore solution was extracted from the slurry of sodium silicate-activated 20/80 slag/Class C fly ash cement by centrifuging slurries at 6000 rpm for 10 min. The pH of extracted pore solution was 13.7. The test samples were prepared in the following manner: first, 0.5 g CMC was immersed into 3 ml pore solution at room temperature; second, pore solution-wetted CMC was autoclaved for 24 h at 85 °C and 200 °C; and, finally the pore solution-treated CMC was dried at 100 °C for further testing.

2.2. Measurements

The molecular weight (MW) of the "as-received" 30, 100, 2000, and 30,000 PA CMCs was measured by High-Performance size-exclusion Chromatography/Laser Light Scattering (HPC/LLS). First, all the CMCs, except for 30,000 PA, were dissolved in running buffer at ~3.5 mg/ml concentration, then filtrated through a 200 nm Dura-pore membrane. The dissolved 30,000 PA formed a large aggregate, precluding its filtration so that there was no possibility to measure its MW. The High-Resolution Scanning Electron Microscopy (HR-SEM) was used to explore the different morphological features of CMCs. TAM Air Isothermal Microcalorimeter was employed to obtain the initial- and final-heat release times and to determine the cumulative heat of hydration evolved during the hydrolysis-hydration of these cementitious slurries at 85 °C. The initial- and final-heat release times were determined at the time of the cross point of extended baseline and the slope lines of the heat flow peak [23]. The total heat, J/g, was computed from the enclosed area of the curve with the baseline made between the initial and final setting times. Microcalorimeter was also used to measure *in-situ* heat evolution in a process of dissolution of sodium silicate activator and reaction products of CMC treated with cement pore solution; self-degradation of CMC-modified cement after contacting water.

The compressive strength for 85 °C–24 h-autoclaved cements was obtained using Instron Model 5967. The cylindrical (16 mm diameter by 35 mm length) specimens were solidified at room temperature for 72 h and autoclaved at 85 °C for this assessment. Some of the 85 °C-cured specimens were further heated at 200 °C for 24 h and their porosity was measured with the helium pycnometer. The measured values provided comparative porosity estimates for samples with different CMCs. The thermal decomposition-related properties of non- and pore solution treated-CMCs were investigated using Thermo Gravimetric Analysis (TGA) at the heating rate of 20 °C/min in a N_2 flow. Pyrolysis–Gas Chromatography/Mass Spectroscopy (Py–GC/MS) was employed to identify and quantify the volatile derivatives emitted by the decomposition of CMC. To accomplish this, a 5–10 mg sample was pyrolyzed at 450 °C by a CDS 2500 Pyrolysis Autosampler, and then, the volatile chemical compounds were identified and quantified using an HP 5890 Series II Gas Chromatograph coupled with an HP 5989 Mass Engine. The chromatographic peaks were identified by referencing them to the NIST MS library and data in the literature, and by comparing their chromatographic retention times to those of the available reference chemical compounds. Some solid compounds remained after CMC decomposition. Fourier Transform Infrared (FT-IR) spectroscopy was adapted to identify them and to define their reaction products with sodium silicate at 200 °C. In preparing the FT-IR samples, the dry mixtures with 100/0, 89/11, 86/14, 80/20, 67/33 CMC/sodium silicate ratios by weight were dissolved in a constant amount of water at room temperature, and then placed in an oven at 200 °C for 24 h; thereafter, the dry samples were ground up for FT-IR analysis.

3. Results and discussion

3.1. CMCs

The viscosities of solutions made by dissolving 1 g CMC in 200 g water were 200, 300, 1010, and 6950 cp for the 30 PA, 100 PA, 2000 PA, and 30,000 PA, respectively, suggesting that the increase in number of PA corresponds to an increasing molecular weight (MW) and rising viscosity, while the pH of all CMCs ranged from 7.45 to 7.87. As expected, the MW of 30 PA, 100 PA, and 2000 PA CMCs determined by HPC/LLC were 80,500, 133,400, and

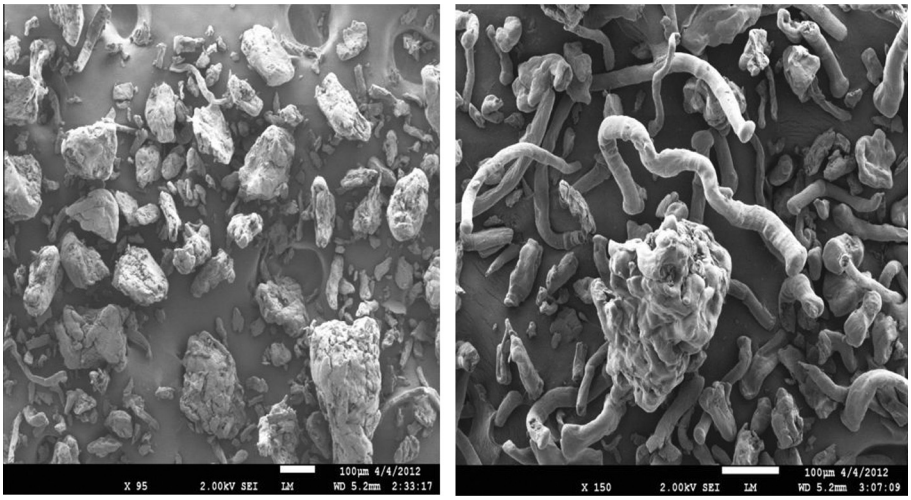

Fig. 1. SEM images of 30 PA (left) and 30,000 PA (right) CMCs.

224,000, respectively. Thus, the MW of 30,000 PA was assumed to be more than 224,000. Fig. 1 shows the SEM image of "as-received" 30 PA and 30,000 PA CMC powders. They disclosed two distinctive micro-structures: One was agglomerated particles with sizes between 10- and 200-µm; the other was a noodle-like conformation.

3.2. Changes in heat-release behaviors of cement slurry by CMCs

Table 1 summarizes the initial and final time of the heat release peak and the total heat evolved, J/g, at 85 °C. The slurry with 30 PA was mixed at two different w/b ratios to evaluate effect of water amount on the time and the amount of the evolved heat. Fig. 2 depicts the microcalorimeter curves in elapsed times up to 14 h after the ampoules containing the slurries with 30 PA-, 100 PA-, 2000 PA-, and 30,000 PA-CMCs were placed in the calorimeter. The reactions of the blend materials with the formation of geopolymer products are complex and include such processes as dissolution, precipitation, polycondensation [24]. Both peaks likely involve precipitation of reaction products; although the first one may be dominated by the reactions of the slag while the second one by the polycondensation of both slag and fly ash [25]. The results suggest that both water-to-blend ratio and the molecular weight of CMCs affected the time of the heat release in calorimetric tests. Increase of w/b ratio for the sample with 30 PA CMC resulted in delayed time of the heat peak and decreased cumulative heat. In the case of the 0.75 w/b ratio tests with 30 and 30,000 PA the difference in the position of the heat peaks, the shape of the curves and total evolved heat was obviously associated with the different CMCs in the systems. Replacement of the low molecular weight CMC with the high molecular weight one delayed the heat peak and more than doubled the amount of the total heat released. Only one peak appeared in the tests with the 30 PA, all other samples showed double peaks.

Table 1
Initial- and final-heat release times and total heat evolved during hydration of 20/80 slag/Class C fly ash ratio sealer slurries containing various CMCs at 85 °C.

CMC (PA)	Water/ blend	Initial heat-release time (h:min)	Final heat-release time (h:min)	Total evolved heat (J/g)
30	0.33	0:50	4:59	113.0
30	0.75	1:17	7:32	26.0
100	0.39	1:36	9:52	99.5
2000	0.51	1:11	6:45	98.3
30,000	0.75	3:13	10:49	63.9

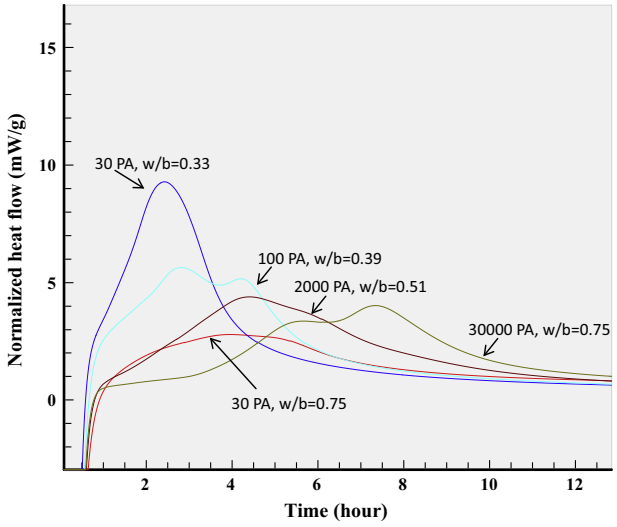

Fig. 2. Microcalorimetric curves at 85 °C of 30, 100, 2000, and 30,000 PA CMC-modified sealer slurries mixed at different water-to-blend (w/b) ratios.

3.3. Compressive strength

Fig. 3 plots the values of compressive strength for cements with the CMCs of different MWs. The data revealed that compressive strength declined with an increase in CMCs' MW accompanied by the increase in the water amount; in fact, the average compressive strength of 18.0 MPa for the cement made with the lowest MW (30 PA) and water-to-blend ratio of 0.33 fell by nearly 39% to 10.1 MPa, when the highest MW CMC (30,000 PA) and w/b ratio of 0.75 was used. For the drilling operations to resume after curing circulation losses the accepted compressive strength is 3.5 MPa [26]. Even the lowest compressive strength achieved with the 30,000 PA was more than sufficient for plugging the fractures and resuming the drilling.

3.4. TGA study

One inevitable factor affecting the self-degradation of cement was the emanation of gaseous species, in particular CO_2 and acetic

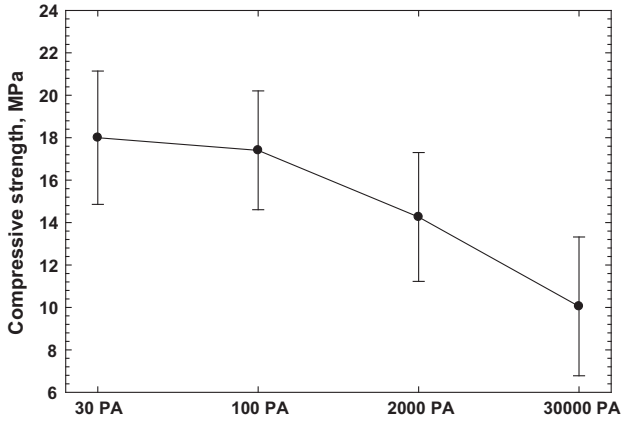

Fig. 3. Compressive strength of 85 °C-autoclaved sealers containing 30, 100, 2000, and 30,000 PA CMC.

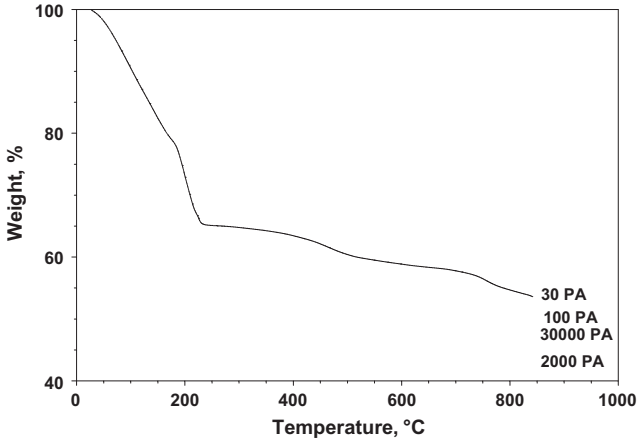

Fig. 5. TGA curves for pH 13.7 pore solution-treated CMCs at 200 °C.

acid, brought about by thermal decomposition of CMC in the cement body. A high rate of such release may improve the self-degrading performance of cement. The other consideration was the exposure of CMC to a highly alkaline environment at elevated temperature, in cement slurries with pH 13.7. As reported [27], treating cellulose with sodium silicate changes its thermal decomposition properties. TGA in a range of 25–850 °C was used to obtain information on the weight loss and thermal decomposition behaviors of various CMCs treated with pH 13.7 pore solution extracted from cement slurry. The treatment was conducted by exposing the CMCs in the pore solution to 200 °C for 24 h. The 200 °C is a common static temperature for EGS wells. For comparison purpose, weight loss and thermal decomposition behaviors of non-treated and 85 °C–24 h-treated CMCs were also investigated. The results reflect effect of both high temperature and alkali environment on CMCs' degradation.

Fig. 4 shows the TGA curves for non-treated 30, 100, 2000, and 30,000 PA CMCs. The features of these curves closely resembled each other for all CMCs, representing two major thermal decomposition stages: first, at ~276 °C; and the second at around 603 °C. At the end testing temperature of 850 °C, the total loss in weight for all CMCs was ~81.4%. When these CMCs were treated with pore solution at 200 °C, their TGA curves revealed three major distinctions from those of non-treated ones (Fig. 5): first, all curves showed one major decomposition pattern, wherein the principal weight loss rapidly progressed at temperatures between 25 °C and 250 °C; second, beyond that, some minor weight losses occurred in two different temperature ranges, ~400 – ~520 °C and ~670 – ~780 °C; and, third, the weight loss at the range of 25 – 850 °C depended on the particular CMC. The weight loss between ~670 and ~780 °C likely involved reaction products of cement species. The first two distinctions strongly suggested that the CMC was very susceptible to a pore solution with a 13.7 pH at 200 °C. Such treatment promoted the alkali-initiated thermal decomposition of CMC. The volatile-products-related weight losses in the temperature range of interest between 25 and 250 °C were 34.2%, 37.5%, 44.5% and 49.1% for 30, 100, 2000 and 30,000 PA respectively.

Fig. 6, based upon the TGA curves, plots the weight loss of CMCs, exposed to cement pore solution, at temperatures ranging from 200 to 350 °C. The weight loss increased with the increased MW of CMCs. CMCs with a high MW produced abundant amounts of volatile derivatives. Conceivably, the magnitude of sealer's self-degradation may depend on the amount of such volatile derivatives emanated in cement, with their large release enhancing the magnitude of degradation. Since a reasonable approximation for the placement temperature of the blend in a geothermal well would be around 85 °C the thermal decomposition behaviors of CMCs treated in pore solution at this temperature were also studied. The resulting TGA curves (not shown) revealed the features similar to those of non-exposed ones, except for a shift in the first decomposition temperature to lower values. For instance, for 30

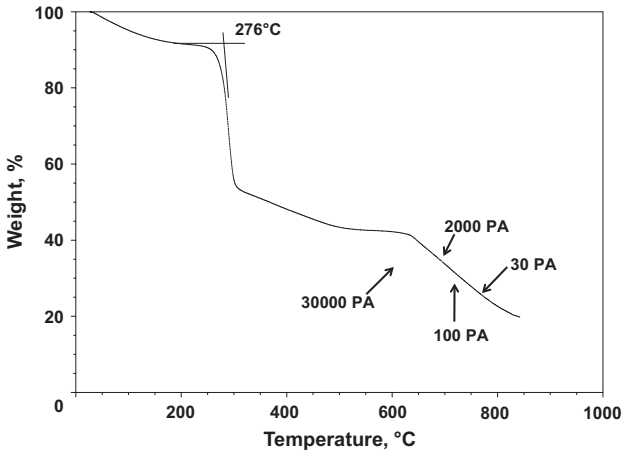

Fig. 4. TGA curves for 30, 100, 2000, and 30,000 PA CMCs.

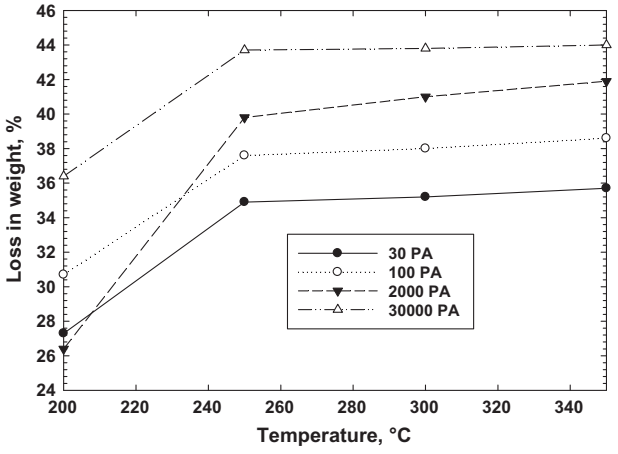

Fig. 6. Loss in weight of 200 °C pore solution-treated CMCs at temperatures 200–350 °C.

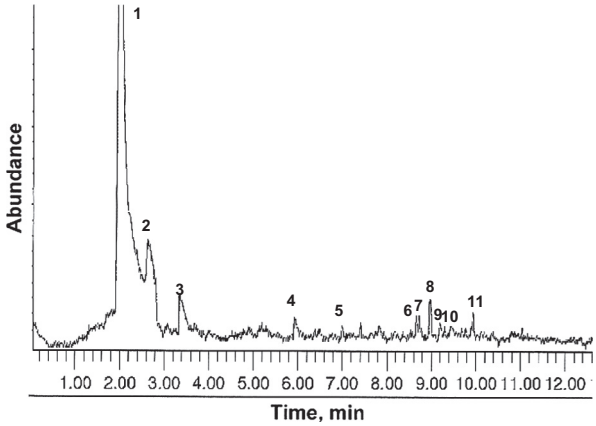

Fig. 7. Py–GC/MS abundance-retention time curve of 450 °C-pyrolyzed 30,000 PA CMC.

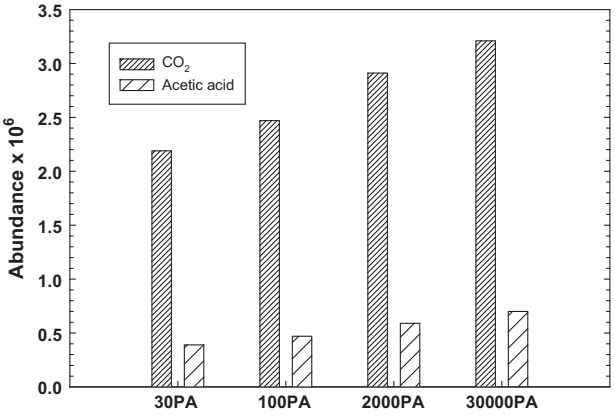

Fig. 8. Abundances of CO_2 and acetic acid emanated from 450 °C-pyrolyzed 30, 100, 2000, and 30,000 PA CMCs.

PA, the first decomposition temperature of non-exposed CMC shifted from 276 °C to 185 °C. The data also demonstrated that the extent of such shift depended on the MW; an increase in MW minimized this shift. Consequently, the difference between shifted and original temperatures was 91, 87, 76, and 74 °C for 30 PA, 100 PA, 2000 PA, and 30,000 PA, respectively, underscoring that the sensitivity of a lower MW CMC to pH 13.7 pore solution at 85 °C was much higher than that of a high MW. In other words, CMC with a high MW possesses a better thermal stability at this placement temperature.

3.5. Pyrolysis–Gas Chromatography/Mass Spectroscopy (Py–GC/MS) study

As mentioned in the TGA study, the thermal decomposition of all pore solution-treated CMCs was characterized by displaying one major decomposition pattern at temperatures from 25 to 850 °C; most of their decomposition was completed at temperatures below 450 °C. Thus identification of volatile derivatives and quantification of the major components released by CMC's thermal decomposition were performed at 450 °C using Py–GC/MS. Fig. 7 shows the abundance-retention time curve for 30,000 PA CMC and Table 2 summarizes the eleven pyrolysis-induced derivatives along with their abundance. Among the main derivatives of CMC were 56.2% CO_2 and acetic acid at 12.3% in conjunction with the minor derivatives comprising 31.5%. Similar results with two major decomposition derivatives, CO_2 and acetic acid, from pyrolyzed CMC, were reported by other investigators [28,29]. Fig. 8 shows the changes in abundance of both CO_2 and acetic acid derivatives at 450 °C as a function of MW. The abundance of these derivatives tended to rise with an increasing MW, implying that CMCs with a high MW emitted more volatile derivatives. In fact, the abundances of CO_2 and acetic acid for 30 PA with the lowest MW of 80,500 were 2.19×10^6 and 0.39×10^6, and these numbers rose by 46.6% and 79.5% to 3.21×10^6 and 0.7×10^6, when the MW was increased to >224,000 (30,000 PA). Thus, this finding strongly supported the earlier TGA data. The CMC with a high MW would generate high amounts of these volatile derivatives in sealer with a high pH, enhancing the cement's self-degradation.

Table 2
Pyrolysis derivatives along with their abundance obtained from Py–GC/MS at 450 °C for 30,000 PA CMC.

ID number	Retention time (min)	Compounds	Abundance $\times 10^6$
1	1.95	Carbon dioxide	3.21
2	2.61	Acetic acid	0.70
3	3.36	1-Hydroxy-2-propanone	0.32
4	5.92	(2-Oxo-3-cyclopenten-1-yl)acetaldehyde	0.20
5	6.99	2-Methyl-2-cyclopenten-1 -one	0.12
6	8.66	2-Hydroxy-3-mehyl-2-cyclopenten-1-one	0.19
7	8.71	3,4,4,-Trimethyl-5-oxo-2-hexenoicacid	0.20
8	8.97	2,4-Dimethyl-1,3-cyclopentanedione	0.28
9	9.19	3-Methyl-phenol	0.14
10	9.45	2-Methyl-phenol	0.11
11	9.94	3-Trans-diethoxy-5-methylcyclohexane	0.24

3.6. Porosity of cement

Fig. 9 shows the porosity of 85 °C-autoclaved cements containing 30, 100, 2000, and 30,000 PA and a control without CMC after heating at 200 °C for 24 h. The porosity of the control cement without CMC was 23.1%. This value increased by 19% to 27.4% when the CMC with the lowest MW (30 PA) was added to the control. A further increase in MW of added CMC caused increase in porosity; the CMC 30,000 PA with the highest MW created 50.5% porosity, which was more than double that of the control. Higher w/b mixing ratio for samples with larger MW CMCs was another likely cause of the increasing porosity. The development of a highly porous structure can be one of the factors promoting the self-degradation of cement. It should be mentioned that the CMC with high molecular weight, 30,000 PA, formed aggregates of limited solubility in water at room temperature. Although the CMC was better dispersed when blended with cement slurries and no CMC aggregates could be seen

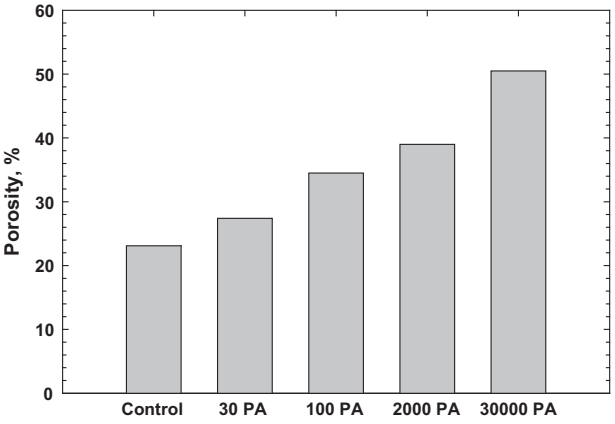

Fig. 9. Porosity of 85 °C-autoclaved cements with and without various CMCs after heating at 200 °C.

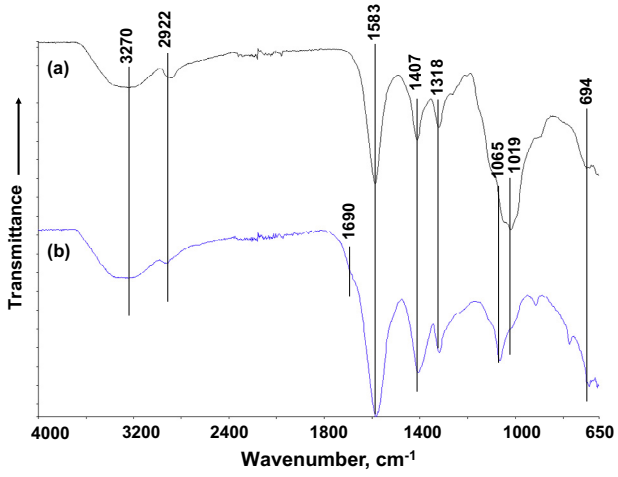

Fig. 10. FT-IR spectra of non-treated (a), and 200 °C-heated CMCs (b).

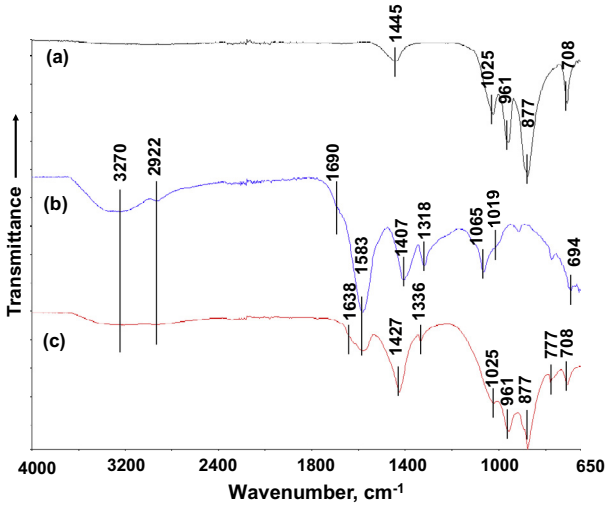

Fig. 12. Comparison of FT-IR spectra of 0/100 (a), 100/0 (b), and 20/80 (c) CMC/sodium silicate samples.

in 85 °C-autoclaved cement the presence of some non-dissolved parts of it in the cement cannot be completely excluded. Decomposition of the non-dissolved 30,000 PA could also contribute to the increased porosity of this cement sample.

3.7. Chemical affinity of CMC with sodium silicate

Although a part of CMC in cement converts to volatile species at 200 °C, the non-volatile CMC remnants might react with hydrolysates derived from the dissolution of sodium silicate in water. To obtain information on these reactions' products solutions of 100/0, 20/80, and 0/100 CMC (30,000 PA)/sodium silicate weight ratios were heated at 200 °C for 24 h to convert them into the solid samples and analyzed with FT-IR.

Fig. 10 illustrates FT-IR spectra in the wavenumber region, 4000–650 cm^{-1}, of non-treated and 200 °C-heated CMC. Based upon the chemical structure of CMC and literature survey [30–33], the absorption bands (a) of the non-treated CMC were attributed as following: the band at 3270 cm^{-1} to OH stretching vibration, at 2922 cm^{-1} – to aliphatic C—H stretching vibrations, at 1583 and 1407 cm^{-1} – to C—O asymmetric and symmetric stretching in the carboxylate ion group, —COO^-, the band at 1318 cm^{-1} was related to C—OH bending, the shoulder at 1065 cm^{-1} referred to ether C—O—C stretching in glucosidic unites, the band at 1019 cm^{-1} was assigned to ether C—O—C stretching in β-(1,4)-glucosidic and —CH_2—O—CH_2-linkage; and the band at 694 cm^{-1} to Na^+—O^- link stretching in sodium alkoxide group. By comparison, the feature of FT-IR spectrum (b) of the 200 °C-heated CMC represented two major differences: one was the changes in the intensity of two ether group-related bands; the other was the appearance of a new shoulder at 1690 cm^{-1}, assigned to C=O stretching in carboxylic acid group, —COOH. For the former difference, the shoulder band at 1065 cm^{-1} became the principal band, whereas the intensity of the band at 1019 cm^{-1} strikingly decayed, suggesting that the C—O—C bonds in β-(1,4)-glucosidic and CH_2—O—CH_2 – linkage were ruptured at 200 °C, while the other ether group in glucosidic unites remained intact. From this information, it is possible to assume that the hydrothermal decomposition of CMC at 200 °C results in two non-volatile derivatives, sodium glycolate and glucosidic acid as shown in Fig. 11.

CMC and sodium silicate reaction products were also identified by FT-IR analysis. Fig. 12 compares the spectral features from 0/100, 100/0, and 20/80 CMC/sodium silicate ratio samples. The spectrum (a) of 200 °C-heated bulk sodium silicate encompassed two silicate-related bands at 1025 and 961 cm^{-1}, corresponding

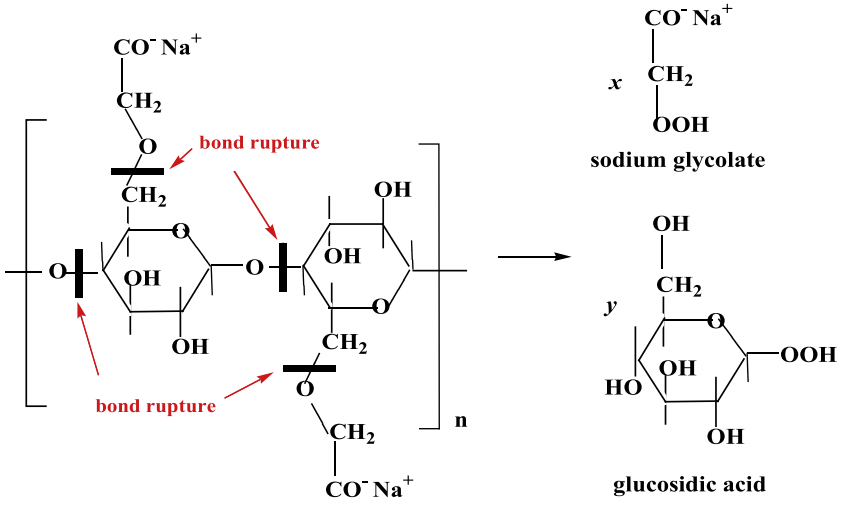

Fig. 11. Hypothetical scheme of CMC hydrothermal decomposition at 200 °C.

to the oxygen-bridging Si—O—Si asymmetric stretching and non oxygen-bridging Si—O^- Na^+ stretching [34,35], and also two carbonate-related bands at 1445 and 708 cm^{-1}, due to CO_3^{2-} possibly in the sodium carbonate [36,37]. Since the dissolution of sodium metasilicate in water introduces two hydrolysates, metasilicic acid, H_2SiO_3 and sodium hydroxide, NaOH, the interactions between these hydrolysates during 200 °C-heating treatment in the presence of an atmospheric CO_2 led to the formation of the sodium polysilicate structure by polycondensation reaction, while the sodium carbonate formed due to the carbonation of NaOH. Fig. 13 shows the proposed hydrolysis, polycondensation, and carbonation reactions of sodium silicate.

When the spectral features (c) of 20/80 ratio sample were compared with those of 0/100 and 100/0 ratios, there were three major differences: first, the carboxylic acid-related band at 1690 cm^{-1} was eliminated; second, the bands at 1407 and 1318 cm^{-1} belonging to the C—O symmetric stretching in the carboxylate ion and the C—OH bending were shifted to 1427 and 1336 cm^{-1}, respectively; and, third was the appearance of new bands at 1638 and 777 cm^{-1}. The first difference suggested that the —COOH groups present in sodium glycolate and glucosidic acid derived from the thermal decomposition of CMC were transformed to —COO^- Na^+ by their reactions with NaOH hydrolysate from sodium silicate [38,39]. On the other hand, a possible interpretation of these new bands was the formation of sodium bicarbonate, $NaHCO_3$, [40,41]. If this latter interpretation is valid, the shifted bands not only were due to the original assignments, but also included the sodium bicarbonates in overlapped bands. Accordingly, the interactions between CMC and sodium silicate at 200 °C may lead to the formation of the following three reaction products, disodium glycolate salt, sodium glucosidic salt, and sodium bicarbonate (Fig. 14), coexisting with some sodium polysilicate and sodium carbonate derivatives from sodium silicate.

The maximum heat evolving when these reaction products formed in cement at 200 °C come in contact with water was evaluated using microcalorimeter (Fig. 15). Sodium silicate and 30,000 PA CMC served as two controls in these tests. The samples were prepared by mixing 15.4 g of the reaction products from 200 °C-dried solutions of CMC/sodium silicate with 74 g water. The sodium silicate without CMC evolved 1.12 W/g MHF, which was 37.5% higher than that of CMC alone, suggesting that sodium polysilicate and sodium carbonate emanate more heat after contact with water than two CMC derivatives, sodium glycolate and glucosidic acid. When 11 wt% of the sodium silicate was replaced with CMC, denoted as 11/89 ratio, the value of MHF rose by 14.5%–1.31 W/g compared with that of 0/100 ratio of CMC/sodium silicate. This finding strongly demonstrated that the reaction products, such as disodium glycolate salt, sodium glucosidic salt, and sodium bicarbonate, were responsible for enhancing heat release. However, the MHF value decreased with further replacement of sodium silicate by CMC, e.g. the MHF value for 33/67 ratio was 4.4% lower than that of 0/100 ratio. In this test series, the 11/89 ratio, which was adapted in this study, resulted in the highest MHF value.

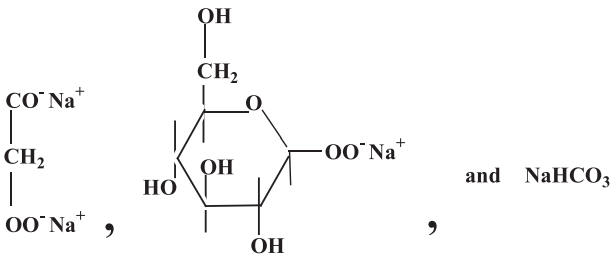

Fig. 14. Products formed in reactions of CMC and sodium silicate at 200 °C.

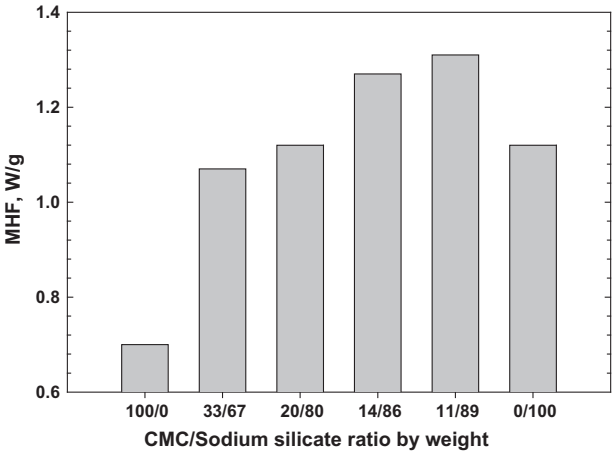

Fig. 15. Maximum heat flow (MHF, W/g) evolved from 200 °C-heated 100/0, 33/67, 20/80, 14/86, 11/89, and 0/100 CMC/sodium silicate samples after mixing with water.

To ensure that the same CMC and sodium silicate reaction products also formed in cement, a sample of 20/80 slag/Class C fly ash ratio cement containing 10% sodium silicate and 1.2% CMC (30,000 PA) by the total weight of cement as described in the Experimental procedure was heated to 200 °C and analyzed using FT-IR. The FT-IR spectrum (not shown) closely resembled that of the sodium silicate/CMC blended sample without cement, except for the domination of slag- and Class C fly ash-related absorption bands in the wavenumbers, ranging from 1300 to 650 cm^{-1}.

3.8. Self-degradation

Two different tests were conducted to visualize and rationalize self-degradation: the determination of the maximum *in-situ* heat energy evolved in the cement after contact with water and visual observation of cement self-degradation after impregnating it with water. In these tests, the 30, 100, 2000, and 30,000 PA CMCs were incorporated into sodium silicate-activated cements. The sodium silicate-activated cement without CMC served as control. The

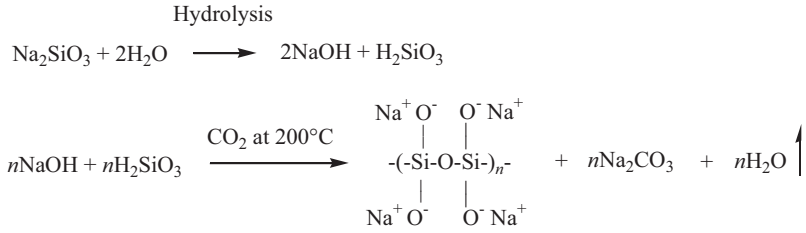

Fig. 13. Sodium silicate reactions during 200 °C heating in atmosphere.

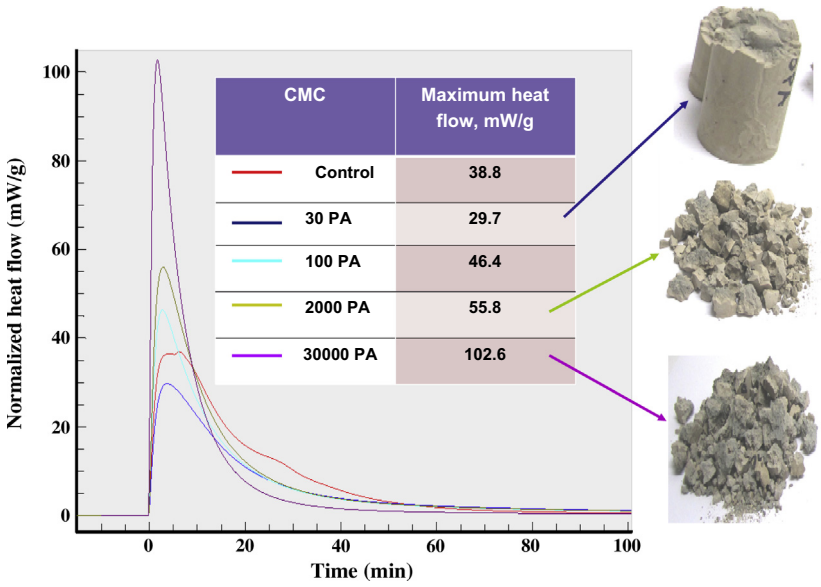

Fig. 16. Comparison of self-degradation performances for cements modified with different CMCs.

detailed test procedures were as follows. For the first test, (1) cement slurry was placed in the glass ampoule, and then autoclaved for 24 h at 85 °C and 6.9 MPa, (2) the cured cement was heated at 200 °C for 24 h, then cooled for 24 h at room temperature, (3) the cooled cement was weighted, and the samples' weights ranged from 9.06 to 9.25 g, (4) 8 g water at 22 °C were poured on the surface of cooled cement, and (5) immediately after the water addition, the ampoule was sealed, and placed in TAM Air Isothermal Microcalorimetry at 22 °C to trace the rate of the heat flow as a function of elapsed time. For the second test, (1) the cement was autoclaved at 85 °C for 24 h under a pressure of 6.9 MPa, (2) the autoclaved cement was heated at 200 °C for 24 h, (3) the hot cement then was left at room temperature for 24 h, (4) after cooling, the cement was placed in a vacuum chamber to remove any air present in the cement, and (5) the air-free cement was impregnated with water, followed by visual observation of the cement's self-degradation.

Fig. 16 depicts the microcalorimeter curves in the elapsed times of up to 100 min for the control, 30-, 100-, 2000-, and 30,000 PA CMC-incorporated cements. For all the samples, the heat flow curve reached the peak within 10 min of the sample introduction into the microcalorimeter. The control sample without CMC had the maximum heat flow (MHF) of 38.8 mW/g, which was related to the dissolution of sodium polysilicate and sodium carbonate compounds derived from the sodium silicate. All the CMCs, except for 30 PA, enhanced the MHF of the cement. The enhancement depended on the MW of CMC; namely, the higher MW resulted in higher *in-situ* heat release. In fact, the sample with the highest MW CMC, 30,000 PA, attained the largest MHF of 102.6 mW/g, corresponding to 2.6-fold increase in comparison with the control. Since the amount of CMC–sodium silicate reaction products rose with an increasing MW, this was likely the main reason of larger heat release for higher MW CMC. The value of MHF was directly correlated with the magnitudes of the self-degradation of the cement. Visual observation from the second test revealed that both the 30,000 and 2000 PA cements contained multiple cracks, compared with 30 PA and the control cements that were only slightly damaged. The samples could be broken further by gentle hand pressure (Fig. 16). As is evident from these images, the 30,000 and 2000 PA cements crumbled very easily. Furthermore, the 30,000 PA CMC-containing cement broke into much smaller fragments than that containing CMC 2000 PA.

4. Conclusions

The studies were aimed at evaluating the usefulness of sodium carboxymethyl cellulose (CMC) as thermally degradable additive in promoting the self-degradation of 200 °C-heated sodium metasilicate-activated slag/Class C fly ash cement system after contact with water and at obtaining the understanding of physicochemical factors contributing to cement's degradation. CMCs of four different molecular weights were explored, 30 PA (80,500 MW), 100 PA (133,400 MW), 2000 PA (224,000 MW), and 30,000 PA (>224,000 MW). The main findings of this work are following.

The CMCs promote self-degradation of the alkali activated slag/Class C fly ash cement system after the slurries cured at 85 °C are heated at 200 °C for 24 h, cooled to room temperature and put in contact with water. The highest tested molecular weight CMC (30,000 PA) added at 1.2% by weight of blend was the most efficient in promoting cement self-degradation among the tested products.

It is believed that the self-degradation is a result of increased cement porosity during the heating period and cement internal heating when in contact with water. Both effects increase with the increasing CMCs' molecular weight and are the most important for the 30,000 PA.

The increased porosity is attributed to the release of gaseous products during the CMC alkali induced decomposition at 200 °C. The major CMC-volatile-degradation product is CO_2 and the minor is acetic acid vapor. The amount of gaseous products formed depended on the CMC's molecular weight and was the largest for the CMC with the highest molecular weight.

The *in situ* cement heating when in contact with water was related to the dissolution of solid products formed during the 200 °C heating. The alkali dissolution and thermal decomposition of CMC produced disodium glycolate salt, sodium glucosidic salt and possibly sodium bicarbonate. In addition sodium polysilicate and sodium carbonate were derived from hydrolysates of sodium silicate at 200 °C. Dissolution of these solid products when in contact with water produced the *in situ* cement heating. The heat evolved was the largest for the high molecular weight CMC, 30,000 PA.

The technical viability of cement slurries required larger water-to-blend ratios for higher MW CMCs. The largest water content likely also contributed to the higher porosity of the 30,000 CMC-containing cement and facilitated cement degradation.

The experimental results suggested that the two factors that played a pivotal role in the self-degradation performance of alkali-activated slag/Class C fly ash blend cement were the development of porous structure and the high heat release arising from the dissolution of abundant CMC and sodium silicate reaction products.

Acknowledgements

The authors would like to acknowledge the funding of the Project by the US Department of Energy Geothermal Technology Program in the Office of Energy Efficiency and Renewable Energy. The authors also would like to thank the Center for Functional Nanomaterials, Brookhaven National Laboratory, which is supported by the U.S. Department of Energy, Office of Basic Energy Sciences, under Contract No. DE-AC02-98CH10886.

References

[1] Kohl T, Megel T. Predictive modeling of reservoir response to hydraulic stimulations the European EGS site Soultz-sous-Forets. In J Rock Mech Min Sci 2007;44:1118–31.
[2] Portier S, Vuataz F, Nami P, Sanjuan B, Gerard A. Chemical stimulation techniques for geothermal wells: experiments on the three-well EGS system at Soultz-sous-Forets, France. Geothermic 2009;38:349–59.
[3] Fabbri F, Vidali M. Drilling mud in geothermal wells. Geothermic 1970;2:735–41.
[4] Sugama T, Kukacka LE, Galen B, Milstone NB. Characteristics of high temperature cementitious lost-circulation control materials for geothermal wells. J Mater Sci 1987;22:63–75.
[5] Irassar EF, Bonavetti VL, Gonzalez M. Microstructural study of sulfate attack on ordinary and limestone Portland cements at ambient temperature. Cem Concr Res 2003;33:31–41.
[6] Van JHP, Visser S. Influence of alkali on the sulphate resistance of ordinary Portland cement mortars. Cem Concr Res 1985;15:485–94.
[7] Sugama T, Brothers L. Sodium-silicate-activated slag for acid-resistant geothermal well cements. J Adv Cem Res 2004;16:77–87.
[8] Sugama T, Brothers L, Van de Putte T. Acid-resistant cements for geothermal wells: sodium silicate activated slag/fly ash blends. J Adv Cem Res 2005;17:65–75.
[9] Nelson E, Barlet-Gouedard V. Thermal cements. In: Nelson E, Guillot D, editors. Well cementing. Sugar Land, USA: Schlumberger; 2006.
[10] Espigares I, Elvira C, Mano JF, Vazquez B, San Roman J, Reis RL. New partially degradable and bioactive acrylic bone cements based on starch blends and ceramic fillers. Biomaterials 2002;23:1883–95.
[11] Boesel LF, Cachinho SCP, Fernands MHV, Reis RL. The in vitro bioactivity of two novel hydrophilic, partially degradable bone cements. Acta Biomater 2007;3:175–82.
[12] Zuo Y, Yang F, Wolka JGC, Li Y, Jansen JA. Incorporation of biodegradable electrospun fibers into calcium phosphate cement for bone regeneration. Acta Biomater 2010;6:1238–47.
[13] Habraken WJEM, Liao HB, Zhang Z, Wolke JGC, Grijpma DW, Mikos AG, et al. In vivo degradation of calcium phosphate cement incorporated into biodegradable microspheres. Acta Biomater 2010;6:2200–11.
[14] Felix Lanao RP, Leeuwenburgh JGC, Wolke JGC, Jansen JA. In vitro degradation rate of apatitic calcium phosphate cement with incorporated PLGA microspheres. Acta Biomater 2011;7:3459–68.
[15] Lopes PP, Garcia MP, Fernandes MH, Fernandes MHV. Acrylic formulations containing bioactive and biodegradable fillers to be used as bone cements: properties and biocompatibility assessment. Mater Sci Eng 2013;C33:1289–99.
[16] Aseyeva RM, Kolosova TN, Lomakin SM, Libonas YY, Zaikov GY, Korshak VV. Thermal degradation of cellulose diacetate. Polym Sci U.S.S.R. 1985;27:1917–26.
[17] Jandura P, Riedl B, Kokta BV. Thermal degradation behavior of cellulose fibers partially esterified with some long chain organic acids. Polym Degrad Stab 2000;70:387–94.
[18] da Conceicao C, Lucena M, de Alencar AEV, Mazzeto SE, de A. Soares S. The effect of additives on the thermal degradation of cellulose acetate. Polym Degrad Stab 2003;80:149–55.
[19] Alldredge AL, Elias M, Gotschalk CC. Effects of drilling mud and mud additives on the primary production of natural assemblages of marine phytoplankton. Mar Environ Res 1986;19:157–76.
[20] Dairanieh IS, Lahalih SM. Novel polymeric drilling mud viscosifiers. Eur Polym J 1988;24:831–5.
[21] Amanullah M, Yu L. Environment friendly fluid loss additives to protect the marine environment from the detrimental effect of mud additives. J Petrol Sci Eng 2005;48:199–208.
[22] Dolz M, Jimenez J, Hernandez MJ, Delegido J, Casanovas A. Flow and thixotropy of non-contaminating oil drilling fluids formulated with bentonite and sodium carboxymethyl cellulose. J Petrol Sci Eng 2007;57:294–302.
[23] Salier Y. Influence du gluconate de sodium et du D75 sur l'hydratation du ciment de classe G. These de doctorat, Universite de Bourgogne; 2008.
[24] Duxson P, Fernandez-Jimenez A, Provis JL, Lukey GC, Palomo A, Van Deventer JSJ. Geopolymer technology: the current state of the art. Advances in geopolymer science and technology. J Mater Sci 2007;42:2917–33.
[25] Kumar S, Kumar R. Mechanical activation of fly ash: effect on reaction, structure and properties of resulting geopolymer. Ceram Int 2011;37:533–41.
[26] Thiercelin M. Mechanical properties of well cements. In: Nelson E, Guillot D, editors. Well cementing. Sugar Land, USA: Schlumberger; 2006.
[27] Tanzos I, Pokal G, Borsa J, Toth T, Schmidt H. The effect of tetramethylammonium hydroxide in comparison with the effect of sodium hydroxide on the slow pyrolysis of cellulose. J Anal Appl Pyrolysis 2003;68–69:173–85.
[28] Jakab E, Meszaros E, Borsa J. Effect of slight chemical modification on the pyrolysis behavior of cellulose fibers. J Anal Appl Pyrolysis 2010;87:117–23.
[29] Torri C, Adamiano A, Fabbri D, Lindfors C, Monti A, Oasmaa A. Comparative analysis of pyrolysate from hebaceous and woody energy crops by Py–GC with atomic emission and mass spectrometric detection. J Anal Appl Pyrolysis 2010;88:175–80.
[30] Ibrahim AA, Adel AM, Abd EI-Wahab ZH, Al-Shemy MT. Utilization of carboxymethyl cellulose based on bean hulls as chelating agent. Synthesis, characterization and biological activity. Carbohydr Polym 2011;83:94–115.
[31] Bao Y, Ma J, Li Na. Synthesis and swelling behaviors of sodium carboxymethyl cellulose-g-poly(AA-co-AM-co-AMPS)/MMT superabsorbent hydrogel. Carbohydr Polym 2011;84:76–82.
[32] Mishar S, Rani GU, Sen G. Microwave initiated synthesis and application of polyacrylic acid grafted carboxymethyl cellulose. Carbohydr Polym 2012;87:2255–62.
[33] Peng H, Ma G, Ying W, Wand A, Huang H, Lei Z. In situ synthesis of polyaniline/sodium carboxymethyl cellulose nanorods for high-performance redox supercapacitors. J Powder Sour 2012;211:40–5.
[34] Farmer VC, Russell JD. The infra-red of layer silicates. Spectrochim Acta 1964;20:1149–73.
[35] Uchino T, Sakka T, Iwasaki M. Interpretation of hydrated states of sodium silicate glasses by infrared and Raman analysis. J Am Ceram Soc 1991;74:306–13.
[36] Soog Y, Goodman AL, McCarthy-Jones JR, Baltrus JP. Experimental and simulation studies on mineral tapping of CO_2 with brine. Energy Convers Manage 2004;45:1845–59.
[37] Trezza MA, Lavat AE. Analysis of the system $3CaO{\cdot}Al_2O_3$–$CaSO_4{\cdot}2H_2O$–$CaCO_3$–H_2O by FT-IR spectroscopy. Cem Concr Res 2001;31:869–72.
[38] Specht CH, Frimmel FH. An in situ ATR–FTIR study on the adsorption of dicarboxylic acids onto kaolinite in aqueous suspensions. Phys Chem Chem Phys 2001;3:5444–9.
[39] Rosenqvist J, Axe K, Sjoberg S, Persson P. Adsorption of dicarboxylates on nano-sized gibbsite particles: effects of ligand structure on bonding mechanisms. Colloids Surf, A 2003;220:91–104.
[40] Chen X, Griesser UJ, Te RL, Pfeiffer RR, Morris KR, Stowell JG, et al. Analysis of the acid-base reactions between solid indomethacin and sodium bicarbonate using infrared spectroscopy, X-ray powder diffraction, and solid-state nuclear magnetic resonance spectroscopy. J Pharm Biomed Anal 2005;38:670–7.
[41] Nyquist RA, Kagel RO. Infrared spectra of inorganic compounds. New York: Academic press; 1973.